ACS APPLIED ENERGY MATERIALS

NTNU

Subscriber access provided by NTNU University Library

Article

Electrolyte Melt Compositions for Low Temperature Molten Carbonate Thermocell

sathiyaraj kandhasamy, Asbjørn Solheim, Signe Kjelstrup, and Geir Martin Haarberg

ACS Appl. Energy Mater., **Just Accepted Manuscript** • DOI: 10.1021/acsaem.8b00984 • Publication Date (Web): 10 Sep 2018

ACS Publications

is published by the American Chemical Society. 1155 Sixteenth Street N.W., Washington, DC 20036

Electrolyte Melt Compositions for Low Temperature Molten Carbonate Thermocell

Sathiyaraj Kandhasamy[†,*], *Asbjørn Solheim*[‡], *Signe Kjelstrup*[§], *and Geir Martin Haarberg*[†]

[†] Department of Materials Science and Engineering, Norwegian University of Science and Technology (NTNU), 7491Trondheim, Norway

[‡] SINTEF Industry, SINTEF, 7491Trondheim, Norway

[§] PoreLab, Department of Chemistry, NTNU, 7491Trondheim, Norway

KEYWORDS: High-temperature thermocells, Molten carbonate electrolyte, Reduced melting point, Multi-component electrolyte, Seebeck Coefficient.

ABSTRACT:

Industrial processes for the production of metals and alloys by metallurgical and electrochemical methods generate a lot of waste heat due to irreversible losses. This waste heat may be used as a power source to generate electricity. A thermocell with non-critical and inexpensive molten carbonate based electrolyte mixtures with reversible ($CO_2|O_2$) gas electrodes was reported recently. It demonstrates the possibility of utilizing the waste heat (> 550 °C) as a power source. Thermocell is an electrochemical cell with two identical electrodes placed in an ionic conducting electrolyte solution with a temperature gradient between the electrodes. The heat source will be used to create the temperature gradient between the electrodes, which will lead to a potential difference by executing ionic diffusion in the electrolyte. In this work, the thermo-physical and chemical properties of the electrolyte mixture were tuned by multi-component mixing with molten (K and Ca) carbonate and LiF additives into the binary (Li,Na) carbonates mixture. It reduces the liquidus temperature to ~ 400 °C and enables the molten carbonate thermocells to recover the high-grade waste heat available at even low temperatures well below 550 °C. Still, the Seebeck coefficient of the thermocells remains large (in the range of -1.5 mV/K).

INTRODUCTION

Many industrial metal production processes require a high temperature operating conditions. Almost half of the heat is emitted as high grade (≥ 400 °C) waste heat into the environment by irreversible losses. The risk of global warming and possible scarcity of the non-renewable energy sources in the near future demands us to use the available waste heat for renewable energy production. Recently, thermocells using symmetrical gas (66 % CO_2 in O_2) electrodes and molten carbonate electrolyte mixtures demonstrated the chance of converting the high grade waste heat (550 - 850 °C) into power.[1-3] One candidate target is waste heat (~ 700 °C) recovery from the industrial silicon-producing furnaces operating at 1800 °C.[2] The electrodes with (CO_2|O_2) gas mixture offer reversibility and fast reactivity with the electrolyte carbonate ions. The change in entropy due to the gas-liquid phase transition of the electrode gas also contributes to the large Seebeck coefficient. The constant supply of the CO_3^{2-} anion source to the melt through the electrode gas mixture keeps the operation continuous. This thermocell shows a predicted increase in the Seebeck coefficient (more negative) with a decrease in the partial pressure of CO_2|O_2 in the electrode gas mixture.[1] This suggests an opportunity to also use the industrial off-gases containing CO_2 and O_2 in mixture with other gases.[1-2]

The melting point of molten carbonate in the electrolyte mixture is the key factor to enable the conditions for thermoelectric conversion. It limits the thermocell operation to be above 550 °C with binary eutectic carbonates. This restricts accessing the waste heat (~ 450 °C) from the industrial aluminum production.[4] The production of aluminum is the second largest amount of metal produced worldwide, next to the iron and steel. At present the primary aluminum is produced by Hall-Héroult electrolysis process[5] with molten cryolite containing the dissolved alumina (Al_2O_3) raw material as an electrolyte. The cells are operated at

temperatures from 950 - 980 °C. Dissolved Al_2O_3 reacts with the consumable carbon anodes to produce aluminum metal along with CO_2 gas:

$$\frac{1}{2}\,Al_2O_3(\text{dissolved}) + \frac{1}{2}\,C(s) = Al(l) + \frac{3}{4}\,CO_2(g) \qquad (1)$$

Nearly 50 % of the input energy is lost as waste heat to the surroundings.[5] As an integral part of the reaction process, the CO_2 gas emission is unavoidable but could be reduced.[6-7] Empowering the molten carbonate thermocells to operate below 450 °C will permit the access to avail the dual sources of waste heat and CO_2-rich off-gases from the industrial aluminum production cells.

Table 1. The melting point and the lattice energy[8] of the molten salts in the electrolyte mixture.

Molten Salt	Melting Point (ºC)	Lattice energy (kJ/mol)
Li_2CO_3	723	2523
Na_2CO_3	851	2301
K_2CO_3	891	2084
$CaCO_3$	825	2804
LiF	845	1030

Table 2. The electrolyte molten melt composition dispersed in 55 vol % of solid MgO.

Electrolyte Mixture	Melt Composition *MX*					Melting Point without MgO from literature (ºC)
	Eutectic Carbonates (mol %)			Addtivies (wt %)		
	Li_2CO_3	Na_2CO_3	K_2CO_3	$CaCO_3$	LiF	
LNC	53	47	---	---	---	496
LNKC	43.5	31.5	25	---	---	397
LNKC-CC	43.5	31.5	25	14	---	376
LNKC-LF	43.5	31.5	25	---	14	368

The lattice structure and ionic arrangement of the molten salts will change during the solid to liquid phase transition due to the dissociation of anion-cation pairs.[9-10] The salt possesses a high electrical conductivity in the molten phase, which increases with the temperature.[11] On the other hand thermal conductivity decreases with increasing temperature. It is thus easier to maintain a stable temperature gradient between the electrodes. The physical properties of the molten salts such as density, viscosity, surface tension, and liquidus temperature are easily tunable by multi-component mixing.[12-15] Addition of new salts with less lattice energy[8] (Table 1) will lower the lattice chemical energy of the mixture and liquidus temperature (Table 2).[13] In addition to the liquidus temperature, the decomposition temperature of the mixture will also be shifted. So, the possible stable temperature window of the electrolyte mixtures in the molten phase is determined by thermal analysis. In the present work we investigate the ternary eutectic $(Li,Na,K)_2CO_3$, with and without $CaCO_3$ and LiF additives, as electrolyte mixture for reduced temperature operation (< 450 °C). The thermocell experiments are conducted with the same conditions as in our previous work,[3] except for difference in electrolyte composition and a wider range of operating temperatures.

EXPERIMENTAL

High purity (> 99%) carbonates of lithium, sodium, potassium and calcium, lithium fluoride and magnesium oxide powders from Sigma-Aldrich were used in electrolyte mixture preparation as purchased. The composition specification of the electrolyte mixtures is listed in Table 2. The mixtures were prepared in a mortar by hand mixing and dried in a hot air oven for 48 h at 200 °C. Pure metal sheet and wire for making the electrodes (Au) and type S thermocouples (Pt-Pt/Rh10%) were purchased from K.A. Rasmussen, Norway. The necessary alumina components for thermocell (Figure 1) construction, like 5-bore tubes (one center bore dia 2.3 mm and four other bores with dia 0.75 mm) and a tubular crucible (inner

diameter of 38 mm with 200 mm length) were bought from MTC Haldenwanger, Germany. The electrodes were made of a gold sheet point-welded to the gold wire inserted into the alumina tubes center bore and the thermocouples (Pt-Pt10%Rh) inserted into two other holes of the tube. The thermocouple junctions were positioned close to the gold electrode to measure the accurate temperature at the electrode surface.

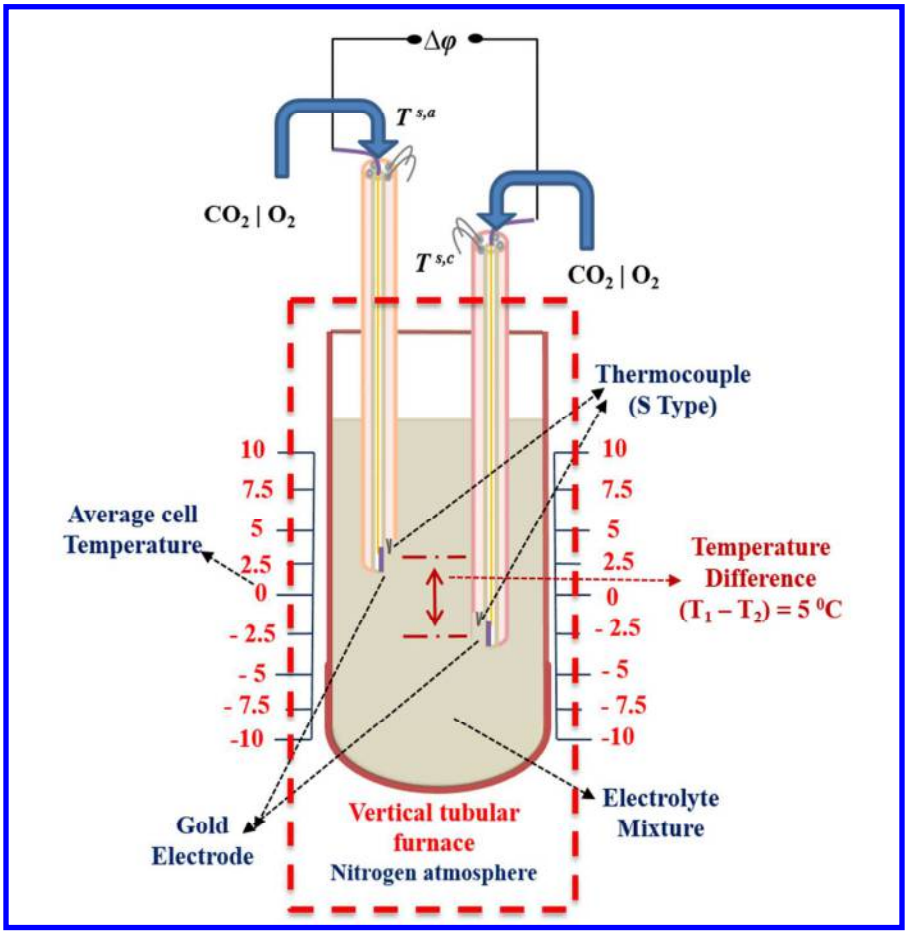

Figure 1. The cross-sectional schematic representation of the molten carbonate thermocell. The electrodes are positioned to establish the temperature gradient of 5 °C, while the cell was maintained at the average cell temperature above the liquidus temperature.

The thermocell was assembled by placing the two alumina tubes (with the electrode and thermocouple) in the cylindrical crucible containing electrolyte mixture. Then the cell was transferred (Figure 1) to a standard laboratory vertical cylindrical furnace under N_2

atmosphere. First, the electrolyte mixture was melted at the average cell temperature in the vertical tube furnace for at least 48 hours to ensure homogeneous melt condition. Pre-mixed 34% oxygen in carbon dioxide gas mixture from AGA, Norway was supplied to electrode tubes at a flow rate of 21 ml/min. The gas mixture flow was controlled by a pair of Brooks instrument Sho-Rate flow meters with ± 5% accuracy. This molten carbonate electrolyte mixture thermocell can be represented as follows:

$$\mathrm{Au}(T^{s,a}) \mid \mathrm{CO_2,O_2(g)} \mid 45\ \mathrm{vol\%\ MX\ (l)},\ 55\ \mathrm{vol\%\ MgO(s)} \mid \mathrm{CO_2,O_2(g)} \mid \mathrm{Au}(T^{s,c}) \quad (2)$$

where MX is the molten salt melt in the electrolyte mixture, listed in Table 2. The reversible ($CO_2|O_2$) gas electrode reaction in the carbonate electrolyte melt is:

$$2\mathrm{CO_2\ (g)} + \mathrm{O_2\ (g)} + 4\ \mathrm{e^-} = 2\ \mathrm{CO_3^{2-}\ (l)} \quad (3)$$

with the reverse reaction at the electrolyte interface of the other electrode.

The electrodes temperature and potential difference were continuously recorded by Agilent, 34972A data acquisition unit. Positioning the electrodes at different heights in the electrolyte creates the temperature gradient (ΔT) between them by the difference in heating zones of the furnace. Meantime the average cell temperature was maintained to be constant. An equilibration time of 15-20 min from the positioning of the electrodes was used to make sure the measured potentials were stable. Then the cell potential was measured at least for 30 mins at each temperature gradient.

The Seebeck coefficient of the thermocell with homogeneous binary electrolyte mixture LNC at the initial state (short time) is:

$$\left(\frac{\Delta\varphi}{(T^{s,c}-T^{s,a})}\right) = \alpha_{s,0} = -\frac{1}{F}\left[\frac{1}{2}S_{CO_2} + \frac{1}{4}S_{O_2} + S_e^* - \frac{1}{2}S_{CO_3^{2-}}^* + \left(\frac{t_2}{x_2} - \frac{t_1}{x_1}\right)\frac{q^*}{T}\right] \quad (4)$$

The Seebeck coefficient of the same LNC electrolyte mixture at steady Soret equilibrium state is:

$$\alpha_{s,\alpha} = -\frac{1}{F}\left[\frac{1}{2}S_{CO_2} + \frac{1}{4}S_{O_2} + S_e^* - \frac{1}{2}S_{CO_3^{2-}}^*\right] \quad (5)$$

where S_j is the entropy of component j at an average temperature of the electrodes T and pressure p_j. The terms S_e^* and $S_{CO_3^{2-}}^*$ are the transported entropies of the electron and carbonate ion, respectively. This equation applies also to multicomponent mixtures.

The entropies and the transported entropies are generally functions of temperature. The gas entropies are expected to be larger than the transported entropies. These terms have then a negative contribution to the Seebeck coefficient. Then t_1, t_2 are the transference coefficients and x_1, x_2 are the mole fractions of Li_2CO_3 and Na_2CO_3. The ratio $\frac{q^*}{T}$ may be interpreted in terms of enthalpy changes across the layer, but it is difficult to interpret the sign of this last term. The last term in the initial state is not included at the Soret equilibrium state. A detailed theoretical derivation of the equations (4 and 5) based on non-equilibrium thermodynamics is explained in our previous work.[1-2] The reported Seebeck coefficients in this paper are considered as to be at initial state, which means the measurement made short time after the establishment of the temperature gradient.

Table 3. Experimental algorithm used for the DSC/TGA thermal analysis.

Segment	Mode	Temperature Range (ºC)	Heating/Cooling Rate (ºC/min)	Hold Time (min)
1	Heating	50 - 300	20	---
2	Isothermal	300	---	10
3	Heating	300 - 530	10	---
4	Heating	530 - 900	20	---
5	Isothermal	900	---	10
6	Cooling	900 - 50	20	---

The chemical and phase stability was analyzed by determining the phase of as-prepared and re-solidified (i.e. before and after thermocell measurement) electrolyte mixture by X-ray diffraction (Bruker-D8 ADVANCE with a CuKα source of λ = 1.5406 Å). The thermal stability and liquidus/solidification temperature of the electrolyte mixtures were determined

by TGA/DSC thermal analysis (NETZSCH STA449C Jupiter). Thermal analysis was performed by heating an alumina pan gently pressed with the powders of as-prepared electrolyte mixture in reference with a similar empty alumina pan under N_2 atmosphere. Different segments of the temperature profile (Table 3) were used to improve the accuracy and minimize the analysis time.

RESULTS AND DISCUSSION

For comparison, the DSC was also performed for pure single lithium carbonate mixture (LC) with 55 vol% solid MgO along with the proposed electrolyte mixtures in Table 2. Figure 2 shows the change in thermal behavior of multi-component mixtures from the pure single salt system. The LC mixture DSC heating curve (Figure 2a) shows a sharp endothermic peak at 718 ºC representing the melting point of the mixture, which is slightly lower than for the pure Li_2CO_3.[16] The presence of solid MgO could help in the early melting of the carbonates due to the decrease in enthalpy of fusion.[14, 17] It suggests that the presence of solid MgO stabilizes the Li_2CO_3 below its liquidus temperature. Then the carbonates begin to melt from the region near the solid MgO surface as an affected solid state in this heterophase mixture.[18]

In all other electrolyte mixtures, a broad endothermic peak covering a wide temperature range with less intensity is observed. The endothermic peak begins once the first liquid is formed and due to the low thermal conductivity of the mixture a wide range of temperature is required to melt the last fraction of carbonates in the mixture. Even two endothermic peaks are seen in the case of LNC and LNKC mixtures. The formation of a metastable solid state by solid-solid phase transformation may lead to an additional endothermic peak before melting.[19] After the solid-solid phase transition the absorption of heat leads to a rapid endothermic peak, which represents the liquidus temperature of the eutectic mixture. Also the

inhomogeneity of the multi-component mixture may lead to an additional endothermic peak. However, the peak maximum is higher than the expected liquidus temperature in Table 2 (molten carbonates without MgO). The large thermal contact resistance between the solid sample and alumina pan container at this heating rate (10 ºC/min) affects the homogeneous temperature distribution in the sample and shifts the melting point.[19] Using a slow heating rate (below 5 ºC/min) may improve the data accuracy.[12]

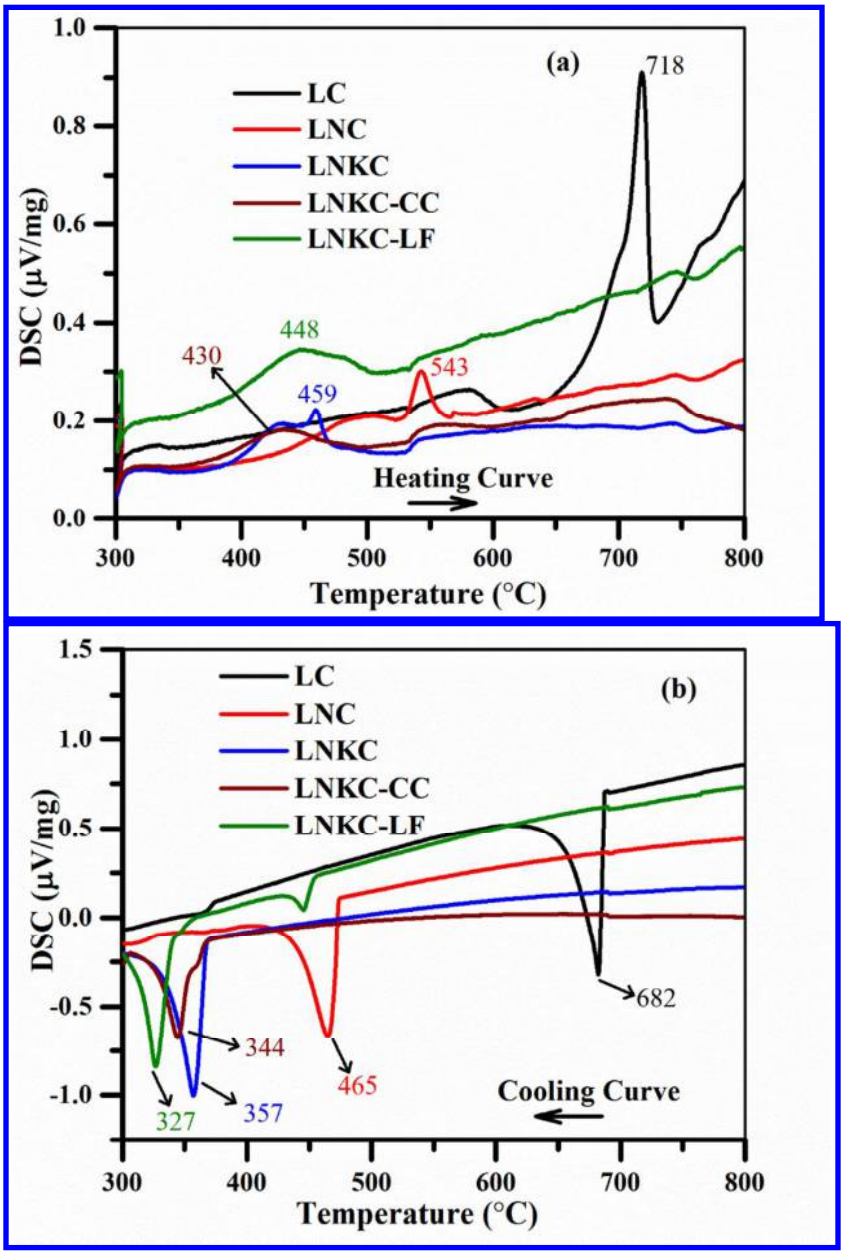

Figure 2. DSC analysis to show the change in **(a)** liquidus and **(b)** solidification temperatures of the electrolyte mixtures in Table 3.

The improved thermal contact between the alumina pan and the sample after melting shows a sharp exothermic peak on resolidification in the DSC cooling curves (Figure 2b). The change in the sharp peak position in the cooling curves confirms the reduction in liquidus temperature in multi-component mixing, in the order of (LC > LNC > LNKC > LNKC-CC > LNKC-LF), this drift is identical to the literature.[13, 20] The steady baseline in the cooling curves displays the enhanced homogeneity[21] after melting. This makes it certain that the melting procedure with average cell temperature for 48h in the tubular furnace before the thermocell measurement will improve the electrolyte melt homogeneity. The presence of the two well distinguishable separate exothermic peaks in the LNKC-LF cooling curve will be discussed later.

The recorded potentials after 20 min of equilibrium time from the establishment of each temperature gradient are shown as raw data in time scale (inset plot in Figure 3a) for the LNKC thermocell. The negative temperature steps show a positive increase in potential which is reversed by reversing the temperature gradient between the electrodes. A negative potential is observed for the thermocell measurements with the hot electrode as a negative terminal. Then the potential changes to positive on reversing the hot and cold electrodes (the positive terminal becomes hot). A negligible bias potential is observed when both the electrodes are close to the average cell temperature (ΔT is ~ 0).[1-2, 22]

The recorded raw data is plotted as potential against the temperature gradient (Figure 3a), and the slope of the straight line determines the Seebeck coefficient. It displays a well-defined thermoelectric condition for the LNKC thermocell at 415 ºC. This behavior is identical to the reports with binary or single carbonate electrolyte mixture at 550 ºC.[1-3] The

thermocell Seebeck coefficients of all the electrolyte mixtures listed in Table 2 are shown in Figure 3b. Lower melting point of the ternary eutectic carbonate electrolyte mixtures makes the thermocell measurement possible at 415 ºC. However, the Seebeck coefficient is also measured at 550 ºC to make a comparative scale with the reported binary LNC electrolyte mixture in identical experimental condition.[3]

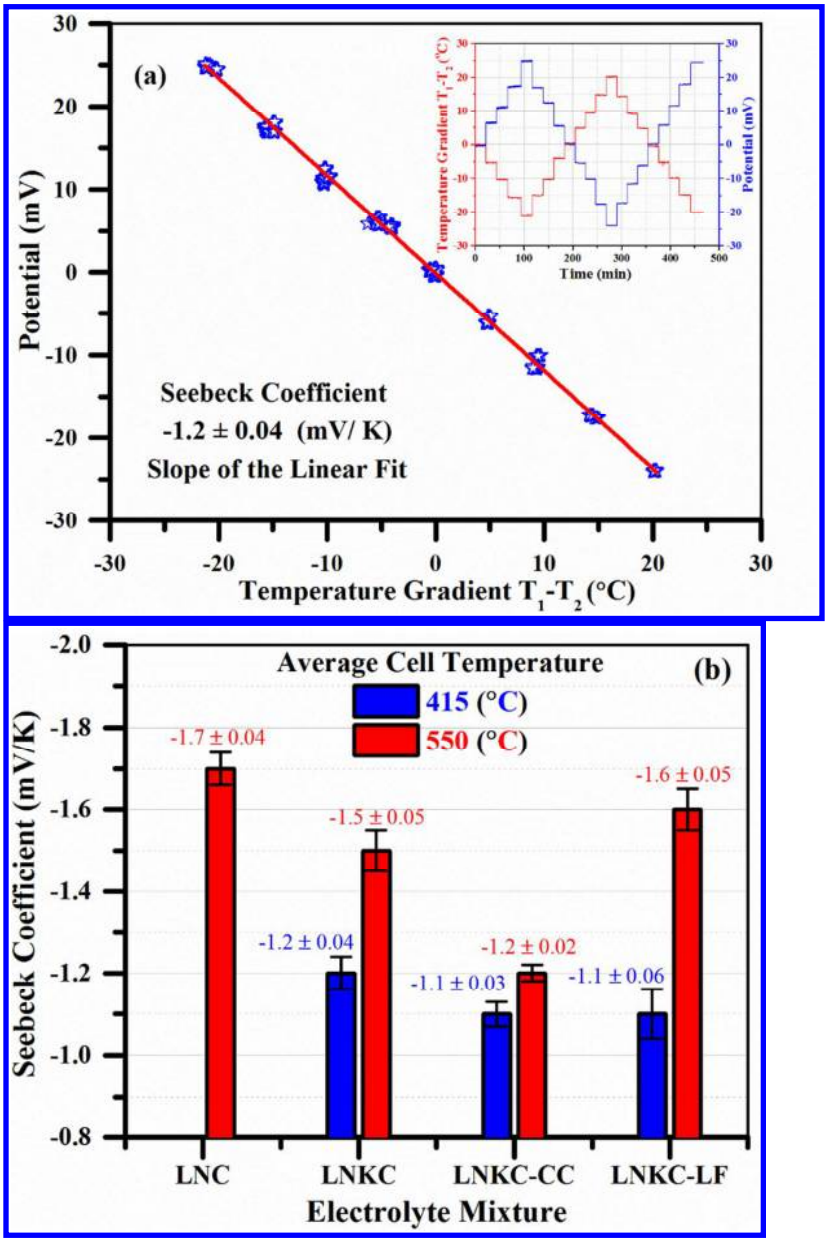

Figure 3. (a) Thermocell measurement with LNKC electrolyte mixture at 415 °C and **(b)** Seebeck coefficient of the thermocells different electrolyte mixtures in Table 2.

The ionic framework and transport behavior of the molten carbonates electrolyte mixture dispersed with solid MgO will be discussed before considering the changes in Seebeck coefficient for different electrolyte mixtures. Mizuhata *et.al.*,[18, 23-24] reported a lower electrical conductivity of similar molten carbonate electrolyte mixtures dispersed with different solid oxides, compared to pure molten carbonates. They also confirmed that the dispersed solid oxide behaves more as an insulator and that the electric conductivity of the mixture depended mostly on the ionic conductivity of the molten phase. The presence of dispersed solid oxide interface influences different transport properties. Nafe[25] supported this observation; the reduction in conductivity of carbonate based composite electrolyte was due to anion-conduction rather than cation on dispersed solid oxides in carbonate melts. In Figure 4, a scheme is proposed to illustrate the ionic environment of the binary molten carbonate electrolyte mixture (LNC) with solid MgO above the liquidus temperature. According to molten salt chemistry, the cation-anion pairs begin to dissociate at the liquid phase transition and increase the ionic degrees of freedom. However, in the liquid phase near the melting point a short-range lattice order remains as a memory effect of the solid lattice.[26-27] Here the cation sits next to the respective anion or vice versa, like in a quasi-crystal.[10, 16] Upon further increase in temperature, the ionic pair dissociation-distance increases and the concentration of ionic charge carriers increases with temperature.[15, 26-28] Reaching the complete dissociation of ion pairs at a higher temperature (boiling point), decomposition will be initiated.[29]

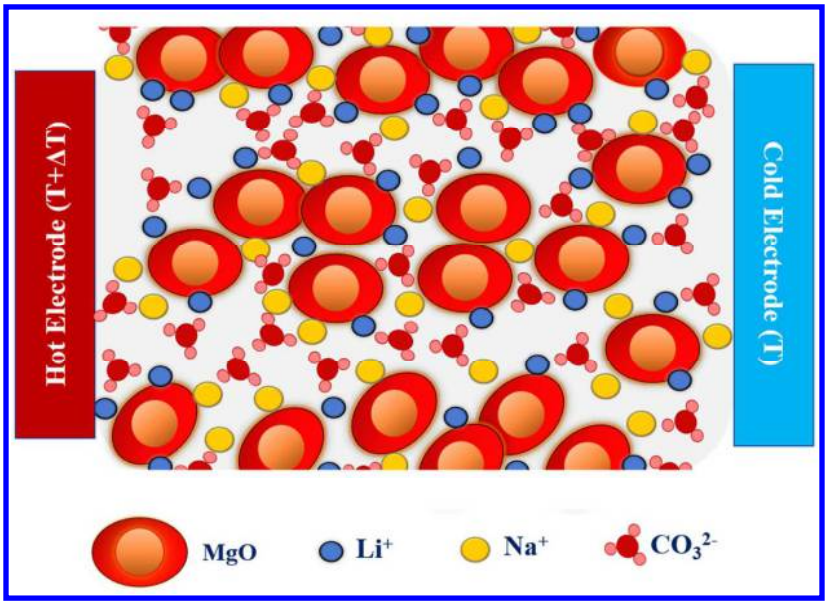

Figure 4. Schematic to illustrate the ionic arrangement in LNC electrolyte mixture at initial condition.

Identical melting behavior is expected in the molten carbonate electrolyte mixtures in thermocells. Ionic movement occurs in electrolyte melt due to thermal diffusion setup by the temperature gradient between the electrodes. In pure molten salts without solid oxide, the fast-moving small cations are the predominant charge carriers rather than the large anions. However the dispersion of solid oxides turns the larger anions into being the charge carriers due to the interface (solid MgO/M^+ cations) composite effect.[25] Thus, the randomly arranged solid MgO particles wrapped with a negative surface charge attract the small metal (Li, Na) cations and withhold its mobility, thus the anions become a dominant carrier. Also, the MgO interface effect on the carbonate melt will reduce the heat flux.[30] The theoretical expression for the Seebeck coefficient of these thermocells derived by irreversible thermodynamics depends on the transported entropy of the carbonate ions, rather than the metal ions, in agreement with the illustrated transport behavior.[1-2] Also, in high-temperature molten carbonate fuel cells with solid oxide matrix and carbonate melt electrolyte, the negative carbonate ions is considered as a major charge carrier.[20, 31]

In this thermocell, the large carbonate anions diffuse from the cold to the hot electrode in the electrolyte mixture. The ionic arrangement in the electrolyte mixture may influence the carbonate ions' degree of diffusion.[15, 25] Even though the cations are immobilized on the solid MgO surface, the addition of larger cations could alter the carbonate ion mobility. The change in anion-cation coulombic force of attraction and polarization power on the change in cation size varies the activation energy for conduction and diffusion of the carbonate ions.[1, 15] The thermocell Seebeck coefficient, directly depends on the transported entropy carried along with the charge carrier (transported entropy is an energy from the lattice order-disorder transition). Thus, the transported entropy of the carbonate ions is reduced while moving from the pure LC to binary LNC electrolyte mixture due to the lattice defects by multi-component mixing and will increase the Seebeck coefficient. But the substitution of sodium cation by large potassium in the binary melt, reduces the Seebeck coefficient.[2] Also in the present study (Figure 3b), the Seebeck coefficient (average cell temperature 550 °C) of the binary LNC thermocell reduces from -1.7 mV/K to -1.5 mV/K for the LNKC. The Seebeck coefficient reduces further to -1.2 mV/K for the electrolyte mixture LNKC-CC due to the strong lattice energy between the asymmetric divalent calcium (Ca^{2+}) cation and carbonate anion in the monovalent cations melt. The LNKC-LF mixture results show a slightly higher Seebeck coefficient than the ternary LNKC mixture, even though the concentration of carbonates is reduced by fluorides addition in the melt. The illustrated ionic framework and the dependency of the Seebeck coefficient on cation composition in the electrolyte mixture, suggest that the preferred path for carbonate ion diffusion is associated with cations that are attracted to the solid MgO surface, rather than to the core of carbonate melt. Mizuhata, et.al.,[18] reported an increase in electrical conductivity upon increasing the amount of solid oxide content, or its surface area in the carbonate melt, which makes the claim reasonable.

A high chemical and phase stability of the dispersed solid MgO in LNC electrolyte melt was reported.[3] The addition of other carbonates into the LNC mixture should retain the stability of the MgO phase.[16-17] The stability of MgO in electrolyte (LNKC-LF) melt with LiF additive is studied by XRD (Figure 5). The sharp and intense diffraction peaks of MgO are at the same position before and after thermocell measurement. But the peaks related to carbonates and fluoride show reduced intensity for the re-solidified electrolyte melt cooled from 550 ºC.[3] Phases other than the phases due to the known melt composition are not observed. The lag in crystallinity on re-solidification from the completely disordered melt phase reduces the diffraction peak intensity of the molten salts. Also, no evidence for recombination of the fluoride anions to the Na/K cations is seen, the strong lattice force of small Li^+ in favors the LiF formation.[32] Meanwhile, the Li^+ rich melt leads to a cation phase separation on re-solidification showing a splitting in peak position corresponding to pure Li_2CO_3 with an additional peak for binary $(Li, Na)_2CO_3$ phase. Such splitting was not observed previously in LNC electrolyte mixture.[3, 32-33] In the LNKC-LF mixture DSC cooling curve, the occurrence of a small additional exothermic peak in the re-solidification range of LNC supports this cation phase separation observed using XRD. However, it couldn't be an impurity phase, thus the multi-component mixing just leads to a doping effect without any chemical side reaction.[13] The solid MgO phase remains stable throughout the thermocell operation even in the presence of LiF in the electrolyte.

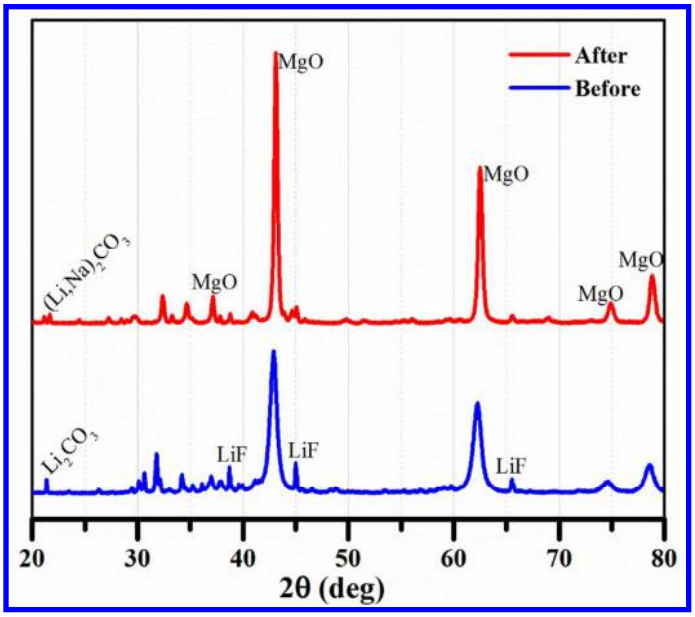

Figure 5. XRD phase analysis of the LNKC-LF electrolyte mixture, before and after the thermocell measurement at 550 °C.

The decomposition temperature of the electrolytes beyond the melting point, where the dissociated CO_3^{2-} ions begin to escape as CO_2 and affects the melt homogeneity,[29] determines the stable liquid phase temperature upper window for the thermocell operation. So, the thermochemical stability of the electrolyte mixtures is analyzed by TGA along with the DSC measurements. In Figure 6 the decomposition process is monitored by measuring the change in electrolyte weight on heating to 900 ºC under N_2 atmosphere. The weight loss observed before 200 ºC is due to the removal of moisture[12] and the sudden drop around 300 ºC is attributed to the implemented isothermal condition followed by the different heating rates used in the measurement algorithm (Table 3). The electrolyte mixtures solid to liquid phase transition shows the respective change in TGA curve around 400 ºC for the ternary carbonate mixtures (LNKC, LNKC-CC, LNKC-LF). As mentioned in the DSC discussion the high interface thermal resistance between the solid sample and alumina pan in high heating rate can shift the corresponding liquid weight change in TGA to high/low temperatures.[12] The lattice energy and cation polarization power of the salt have strong effects on their thermal

stability.[34] As shown in Table 1, the larger lattice energy of the $CaCO_3$ prompts the early decomposition in LNKC-CC.[21, 32] However, the presence of Na, K carbonates with low lattice and ionization energies establishes a short range of stable melt phase in LNKC-CC between the melting and decomposition temperatures.[35] The ternary eutectic carbonate electrolyte mixtures with and without LiF offer a chemical stability at higher temperatures along with the reduced liquidus temperature.[13-14]

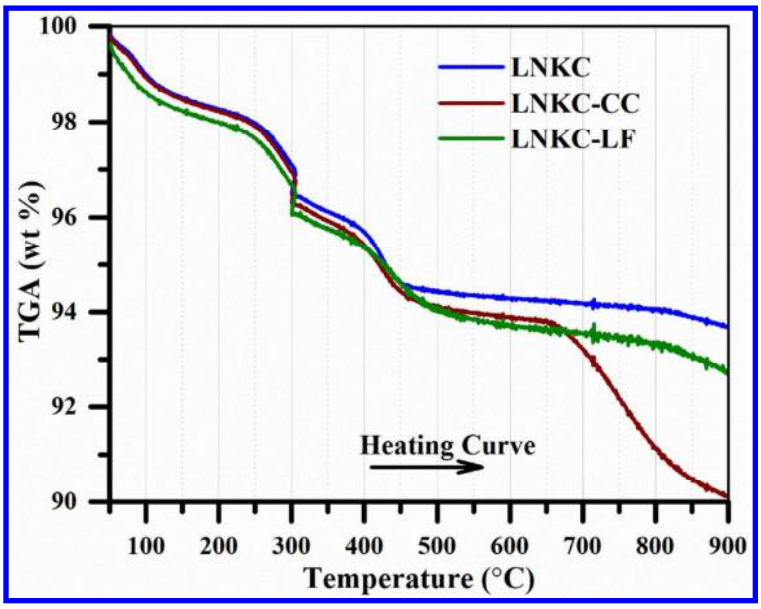

Figure 6. Thermochemical stable of the different electrolyte mixtures by TGA analysis.

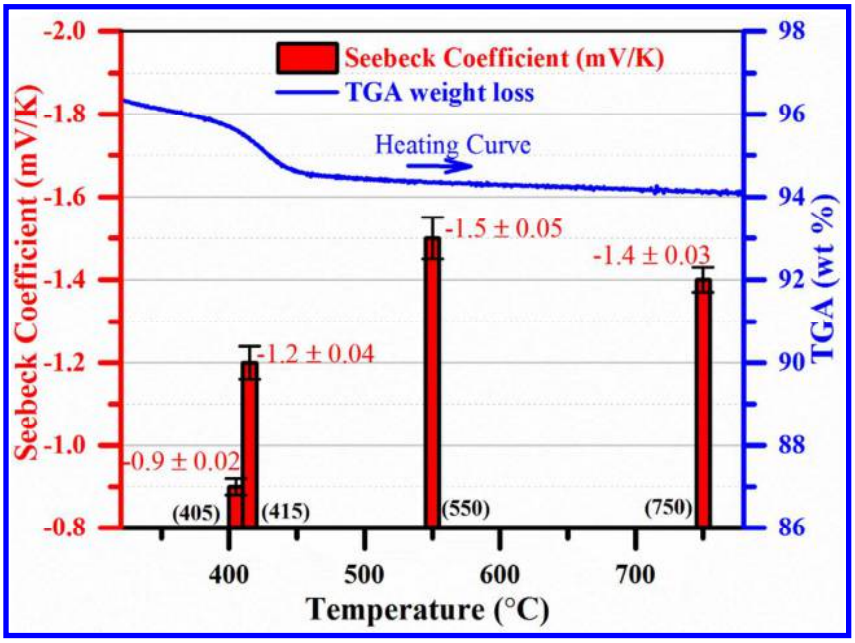

Figure 7. Seebeck coefficient of the LNKC thermocell at different average cell temperatures merged with the TGA weight loss profile.

The thermocell measurements with LNKC ternary molten carbonate electrolyte mixture were performed in the determined stable temperature window (from 405 to 750 ºC). Along with the Seebeck coefficients, the TGA weight loss of the corresponding electrolyte mixture on increase in temperature is also merged in Figure 7. An increase in the carbonate ion degree of freedom by enhanced cation-anion pair dissociation by raising the thermocell temperature lowers the activation energy required for carbonate ion migration.[25, 28] Also the transported entropy of carbonate ions reduces due to large lattice disorder by an increase in the average cell temperature. Thus, the Seebeck coefficient increases from -0.9 mV/K (405 °C) to -1.5 mV/K (550 °C). The dependence of the Seebeck coefficient on the operating temperature is similar to the behavior reported previously (increase in Seebeck coefficient with average cell temperature).[2] Existence of short-range lattice order (quasi-crystalline nature)[33] in the melt phase near the liquidus temperature results in a drastic change in Seebeck coefficient for a small raise (10 ºC) with the average cell temperature (405 to 415 ºC). The further increase in thermocell temperature to 750 ºC, slightly reduces the Seebeck coefficient to -1.2 mV/K.

There is no significant decomposition weight loss observed during TGA measurement under N_2 atmosphere at this temperature. But during the thermocell measurements, the availability of O_2 electrode-gas along with CO_2 could initiate carbonate decomposition a bit earlier, around 730 ºC.[14] Then the dissociated CO_3^{2-} ions begin to escape as CO_2 and affects the homogeneity of the electrolyte mixture by decrease in CO_3^{2-} ions concentration and reduced Seebeck coefficient at 750 °C. However, the LNKC mixture enables thermocell operation at 405 ºC which is well below the desired reduced temperature (450 ºC). The electrolyte mixture with LiF will likely corrode the metal electrodes which demands an extensive study for higher temperature operation,[36] but the gold and platinum metals are stable in this regards. The morphology of the Au electrodes is not modified during the thermocell measurements. Also change in electrolyte composition has no impact on the surface morphology of the Au electrodes. The SEM images showing the surface morphology of the electrodes are provided in the supporting information. Also, the addition of the low melting temperature salts like molten chlorides, nitrates, and hydroxides will liquidize the ternary carbonate mixture even sooner, but the complex ionic melt will affect the solid MgO phase and melt chemical stability.[14, 32, 35]

CONCLUSIONS

A low liquidus temperature of the ternary eutectic LNKC electrolyte mixture can be achieved by multi-component mixing with low lattice energy salts. This permits the operation of molten carbonate thermocell at a reduced temperature range (< 450 ºC). The high-temperature thermochemical stability of the mixture widens the operating temperature window of the thermocell. Addition of $CaCO_3$ and LiF into the ternary eutectic carbonates shifts the liquid phase-transition to even lower temperatures. But the higher lattice energy of $CaCO_3$ brings down the stable temperature window by early decomposition. While the LiF-

addition demonstrates a better stability at high-temperatures, the corrosion effect of the electrodes and other cell components should be investigated before warranting the better performance. XRD analysis shows that the dispersed solid MgO remains stable in LNKC-LF electrolyte at 550 ºC. Thus, the stable and suitable reduced temperature is optimized for the molten carbonate thermocell operation to recover the waste heat (< 450 ºC) from primary aluminum production industries.

AUTHOR INFORMATION

Corresponding Author

*Email: k.sathiyaraj14@gmail.com; sathiyaraj.kandhasamy@ntnu.no

Funding Sources

This research project no. 228296 is financial supported by the Research Council of Norway under ENERGIX program.

ACKNOWLEDGMENT

The authors wish to acknowledge the Research Council of Norway for financial support of the research project “Sustainable and Energy Efficient Electrochemical Production and Refining of Metals (SUPREME)” project no. 228296 and the industrial partners Hydro Aluminium, Boliden, Glencore, and Permascand for support. Kjelstrup is thanking the Research Council of Norway for is Center of Excellence Funding scheme for Porelab, project no. 262644.

REFERENCES

(1) Børset, M. T.; Kang, X.; Burheim, O. S.; Haarberg, G. M.; Xu, Q.; Kjelstrup, S., Seebeck Coefficients of Cells with Lithium Carbonate and Gas Electrodes. *Electrochim Acta* **2015,** *182*, 699-706.

(2) Kang, X.; Borset, M. T.; Burheim, O. S.; Haarberg, G. M.; Xu, Q.; Kjelstrup, S., Seebeck Coefficients of Cells with Molten Carbonates Relevant for the Metallurgical Industry. *Electrochim Acta* **2015,** *182*, 342-350.

(3) Kandhasamy, S.; Calandrino, L.; Burheim, O. S.; Solheim, A.; Kjelstrup, S.; Haarberg, G. M., Influence of Electrode Gas Flow Rate and Solid Oxide Ratio in Electrolyte on the Seebeck Coefficient of Molten Carbonate Thermocell. *J Electrochem Soc* **2017,** *164*, H5271-H5276.

(4) Nowicki, C.; Gosselin, L., An Overview of Opportunities for Waste Heat Recovery and Thermal Integration in the Primary Aluminum Industry. *Jom-Us* **2012,** *64*, 990-996.

(5) Fellner, P.; Haarberg, G. M.; Hives, J.; Kvande, H.; Sterten, A.; Thonstad, J., *Aluminium Electrolysis: Fundamentals of the Hall-Héroult Process*. Beuth Verlag GmbH: 2011.

(6) Welch, B.; Iffert, M.; Skyllas-Kazacos, M., Applying Fundamental Data to Reduce the Carbon Dioxide Footprint of Aluminum Smelters. *Jom-Us* **2008,** *60*, 17-24.

(7) Agnihotri, A.; Rai, S.; Warhadpande, N., Carbon Dioxide Management—Aluminium Industry Perspective. In *Carbon Utilization*, Goel, M.; Sudhakar, M., Eds. Springer Singapore: Singapore, 2017; pp 217-229.

(8) Lide, D. R., *CRC Handbook of Chemistry and Physics, 88th Edition*. Taylor & Francis: 2007.

(9) Okazaki, S.; Matsumoto, M.; Okada, I., Study of Rotational and Vibrational Relaxation of the CO_2^{-3} Ion in Molten Alkali Carbonates by Raman Spectroscopy. *Molecular Physics* **1993,** *79*, 611-621.

(10) Janz, G. J.; Saegusa, F., Molten Carbonates as Electrolytes - Viscosity and Transport Properties. *J Electrochem Soc* **1963,** *110*, 452-456.

(11) Kojima, T.; Miyazaki, Y.; Nomura, K.; Tanimoto, K., Electrical Conductivity of Molten Li_2CO_3-X_2CO_3 (X: Na, K, Rb, and Cs) and Na_2CO_3-Z_2CO_3 (Z: K, Rb, and Cs). *J. Electrochem. Soc.* **2007,** *154*, F222-F230.

(12) Glenn, M. J.; Allen, J. A.; Donne, S. W., Thermal Investigation of a Doped Alkali-Metal Carbonate Ternary Eutectic for Direct Carbon Fuel Cell Applications. *Energ Fuel* **2015,** *29*, 5423-5433.

(13) Zhang, Z. L.; Yuan, Y. P.; Zhang, N.; Sun, Q. R.; Cao, X. L.; Sun, L. L., Thermal Properties Enforcement of Carbonate Ternary via Lithium Fluoride: A Heat Transfer Fluid for Concentrating Solar Power Systems. *Renew Energ* **2017,** *111*, 523-531.

(14) Olivares, R. I.; Chen, C.; Wright, S., The Thermal Stability of Molten Lithium–Sodium–Potassium Carbonate and the Influence of Additives on the Melting Point. *Journal of Solar Energy Engineering* **2012,** *134*, 041002.

(15) Kojima, T.; Miyazaki, Y.; Nomura, K.; Tanimoto, K., Physical Properties of Molten Li_2CO_3-Na_2CO_3 (52:48 mol%) and Li_2CO_3-K_2CO_3 (62:38 mol%) Containing Additives. *J. Electrochem. Soc.* **2013,** *160*, H733-H741.

(16) Janz, G. J., Molten Carbonate Electrolytes as Acid-Base Solvent Systems. *J Chem Educ* **1967,** *44*, 581-590.

(17) Frangini, S.; Scaccia, S., Thermal Stability and Oxidizing Properties of Mixed Alkaline Earth-Alkali Molten Carbonates: A Focus on the Lithium-Sodium Carbonate Eutectic System with Magnesium Additions. *Thermochim Acta* **2013,** *574*, 55-62.

(18) Mizuhata, M.; Harada, Y.; Cha, G. J.; Beleke, A. B.; Deki, S., Physicochemical Properties of Molten Alkali Metal Carbonates Coexisting with Inorganic Powder. *J Electrochem Soc* **2004,** *151*, E179-E185.

(19) Wang, T.; Mantha, D.; Reddy, R. G., Novel High Thermal Stability LiF–Na_2CO_3–K_2CO_3 Eutectic Ternary System for Thermal Energy Storage Applications. *Solar Energy Materials and Solar Cells* **2015,** *140*, 366-375.

(20) Frangini, S.; Masi, A., Molten Carbonates for Advanced and Sustainable Energy Applications: Part I. Revisiting Molten Carbonate Properties from A Sustainable Viewpoint. *Int J Hydrogen Energ* **2016,** *41*, 18739-18746.

(21) Frangini, S.; Scaccia, S., Influence of Lanthanum Carbonate Additions on Thermal Stability of Eutectic Lithium–Sodium Carbonate Near its Melting Point. *Thermochim Acta* **2013,** *551*, 33-39.

(22) Bonetti, M.; Nakamae, S.; Roger, M.; Guenoun, P., Huge Seebeck Coefficients in Nonaqueous Electrolytes. *J Chem Phys* **2011,** *134*, 114513.

(23) Mizuhata, M.; Ohashi, T.; Beleke, A. B., Electrical Conductivity of the Coexisting System Containing Molten Carbonates and Rare-earth Oxide. In *Molten Salts and Ionic Liquids 17*, Fox, D. M.; Mizuhata, M.; DeLong, H. C.; Mantz, R. A.; Trulove, P. C., Eds. 2010; Vol. 33, pp 439-447.

(24) Mizuhata, M.; Ohashi, T.; Beleke, A. B., Electrical Conductivity and Related Properties of Molten Carbonates Coexisting with Ceria-Based Oxide Powder for Hybrid Electrolyte. *Int J Hydrogen Energ* **2012,** *37*, 19407-19416.

(25) Nafe, H., Conductivity of Alkali Carbonates, Carbonate-Based Composite Electrolytes and IT-SOFC. *Ecs J Solid State Sc* **2014,** *3*, N7-N14.

(26) Cornwell, K., The Thermoelectric Potential of Molten Salt Thermocells. *Journal of Physics D: Applied Physics* **1972,** *5*, 1199-1211.

(27) Cornwell, K., The Possibility of using Molten Salts for Thermoelectric Generation. *Journal of Physics D: Applied Physics* **1968,** *1*, 173-178.

(28) Yang, C.; Takagi, R.; Kawamura, K.; Okada, I., Internal Cation Mobilities in the Molten Binary System Li_2CO_3-K_2CO_3. *Electrochim Acta* **1987,** *32*, 1607-1611.

(29) Janz, G. J.; Lorenz, M. R., Molten Carbonate Electrolytes - Physical Properties, Structure, and Mechanism of Electrical Conductance. *J Electrochem Soc* **1961,** *108*, 1052-1058.

(30) Gokon, N.; Nakano, D.; Inuta, S.; Kodama, T., High-Temperature Carbonate/MgO Composite Materials as Thermal Storage Media for Double-Walled Solar Reformer Tubes. *Sol Energy* **2008,** *82*, 1145-1153.

(31) Dicks, A. L., Molten Carbonate Fuel Cells. *Curr Opin Solid St M* **2004,** *8*, 379-383.

(32) Sang, L. X.; Cai, M.; Zhao, Y. B.; Ren, N.; Wu, Y. T.; Burda, C., Mixed Metal Carbonates/Hydroxides for Concentrating Solar Power Analyzed with DSC and XRD. *Solar Energy Materials and Solar Cells* **2015,** *140*, 167-173.

(33) Bates, J. B.; Boyd, G. E.; Brooker, M. H.; Quist, A. S., Raman Spectra of Molten Alkali-Metal Carbonates. *J Phys Chem-Us* **1972,** *76*, 1565-1571.

(34) Pfleger, N.; Bauer, T.; Martin, C.; Eck, M.; Worner, A., Thermal Energy Storage - Overview and Specific Insight into Nitrate Salts for Sensible and Latent Heat Storage. *Beilstein J Nanotechnol* **2015,** *6*, 1487-97.

(35) Chen, C. L.; Tran, T.; Olivares, R.; Wright, S.; Sun, S. Y., Coupled Experimental Study and Thermodynamic Modeling of Melting Point and Thermal Stability of Li_2CO_3-Na_2CO_3-K_2CO_3 Based Salts. *Journal of Solar Energy Engineering-Transactions of the Asme* **2014,** *136*, 031017.

(36) Kawase, M.; Mugikura, Y.; Izaki, Y.; Watanabe, T.; Ito, Y., Effects of Fluoride on the Performance of MCFCs. *J Power Sources* **2003,** *124*, 52-58.

TOC Graphic